Bioenergetic remodeling of heart during treatment of spontaneously hypertensive rats with enalapril

S. C. Leary, D. Michaud, C. N. Lyons, T. M. Hale, T. L. Bushfield, M. A. Adams and C. D. Moyes

Am J Physiol Heart Circ Physiol 283:H540-H548, 2002. First published 18 April 2002; doi:10.1152/ajpheart.00032.2002

AJP - Heart and Circulatory Physiology publishes original investigations on the physiology of the heart, blood vessels, and lymphatics, including experimental and theoretical studies of cardiovascular function at all levels of organization ranging from the intact animal to the cellular, subcellular, and molecular levels. It is published 12 times a year (monthly) by the American Physiological Society, 9650 Rockville Pike, Bethesda MD 20814-3991. ISSN: 0363-6135, ESSN: 1522-1539. Visit our website at http://www.the-aps.org/.

Am J Physiol Heart Circ Physiol 283: H540–H548, 2002.
First published April 18, 2002; 10.1152/ajpheart.00032.2002.

Bioenergetic remodeling of heart during treatment of spontaneously hypertensive rats with enalapril

S. C. LEARY,[1] D. MICHAUD,[1] C. N. LYONS,[1] T. M. HALE,[2]
T. L. BUSHFIELD,[2] M. A. ADAMS,[2] AND C. D. MOYES[1]
Departments of [1]Biology and [2]Pharmacology and Toxicology, Queen's University, Kingston, Ontario, Canada K7L 3N6

Received 16 February 2002; accepted in final form 11 April 2002

Leary, S. C., D. Michaud, C. N. Lyons, T. M. Hale, T. L. Bushfield, M. A. Adams, and C. D. Moyes. Bioenergetic remodeling of heart during treatment of spontaneously hypertensive rats with enalapril. *Am J Physiol Heart Circ Physiol* 283: H540–H548, 2002. First published April 18, 2002; 10.1152/ajpheart.00032.2002.—We used spontaneously hypertensive rats to study remodeling of cardiac bioenergetics associated with changes in blood pressure. Blood pressure was manipulated with aggressive antihypertensive treatment combining low dietary salt and the angiotensin-converting enzyme inhibitor enalapril. Successive cycles of 2 wk on, 2 wk off treatment led to rapid, reversible changes in left ventricular (LV) mass (30% change in <10 days). Despite changes in LV mass, specific activities of bioenergetic (cytochrome-*c* oxidase, citrate synthase, lactate dehydrogenase) and reactive oxygen species (ROS) (total cellular superoxide dismutase) enzymes were actively maintained within relatively narrow ranges regardless of treatment duration, organismal age, or transmural region. Although enalapril led to parallel declines in mitochondrial enzyme content and ventricular mass, total ventricular mtDNA content was unaffected. Altered enzymatic content occurred without significant changes in relevant mRNA and protein levels. Transcript levels of gene products involved in mtDNA maintenance (Tfam), mitochondrial protein degradation (LON protease), fusion (fuzzy onion homolog), and fission (dynamin-like protein, synaptojanin-2α) were also unchanged. In contrast, enalapril-mediated ventricular and mitochondrial remodeling was accompanied by a twofold increase in specific activity of catalase, an indicator of oxidative stress, suggesting that rapid cardiac adaptation is accompanied by tight regulation of mitochondrial enzyme activities and increased ROS production.

hypertension; mitochondria; mitochondrial deoxyribonucleic acid; angiotensin-converting enzyme inhibitor; spontaneously hypertensive rats; cytochrome oxidase; oxidative stress

CARDIAC HYPERTROPHY IS PART of the compensatory response to increased pressure or volume work. Cardiac remodeling in response to hypertension involves complex signaling pathways including mechanical (32) and neural/humoral (18) elements. In the absence of treatment, hypertensive hypertrophy can lead to cardiac failure. Treatment, which typically targets signaling pathways involving ANG II or its receptor AT_1 (18), leads to reductions in cardiac work and results in remodeling of cardiomyocyte architecture and contractile properties (8, 12, 15, 22, 28, 33).

Although most studies assessing the cardiac response to hypertension or its treatment focus on the contractile machinery, bioenergetic compensation must also be integrated into cardiac adaptation (41). Most of the energy required for cardiac work is derived from mitochondrial oxidative phosphorylation. As cardiomyocytes decrease in size, the cells must also reduce mitochondrial content in parallel to preserve bioenergetic regulatory relationships and meet constraints on intracellular space. Failure to make appropriate changes in qualitative and quantitative properties of mitochondria has the potential to alter energy metabolism or accelerate reactive oxygen species (ROS) production. Quantitative and qualitative changes in mitochondria are seen in a number of models of hypertension and cardiac hypertrophy (3, 4, 7, 26, 27, 35, 36, 39). Treatment of hypertension also leads to changes in metabolic characteristics including antioxidant defenses (12) and mitochondrial properties (15, 33). For the most part, the genetic and regulatory mechanisms underlying remodeling of bioenergetics during ventricular hypertrophy and regression remain largely unknown.

Alterations in mitochondrial properties during changes in ventricular mass could arise through altered rates of synthesis or degradation. Few links have been established between the primary signals (mechanoreceptors or neurohumororeceptors) and genes encoding mitochondrial proteins. Presumably, the genetic mechanisms by which hypertension induces hypertrophy are reversed during antihypertensive treatment, but whether such decreases in synthesis account for mitochondrial losses is unclear. Mitochondrial degradation is mediated by protein-specific pathways involving intramitochondrial proteases (6) and organelle-specific pathways involving autophagy by lysosomes (21). The relative importance of the various synthetic and degradative influences during hypertrophic regression remains equivocal.

In the present study, we used spontaneously hypertensive rats (SHR) to investigate the changes in a

Address for reprint requests and other correspondence: C. D. Moyes, Dept. of Biology, Queen's Univ., Kingston, ON, Canada K7L 3N6 (E-mail: moyesc@biology.queensu.ca).

The costs of publication of this article were defrayed in part by the payment of page charges. The article must therefore be hereby marked "*advertisement*" in accordance with 18 U.S.C. Section 1734 solely to indicate this fact.

broad spectrum of mitochondrial structural and functional parameters. Relying exclusively on SHR, we avoided assumptions about genetic relatedness of SHR and normotensive Wistar-Kyoto strains (5). In addition to the age-dependent progression of hypertension inherent in SHR, we incorporated an aggressive antihypertensive treatment to induce rapid changes in ventricular remodeling. Our analyses examined mtDNA copy number, transcription/replication factors, metabolic enzymes, mitochondrial proteases, and putative mediators of mitochondrial fusion and fission. We also examined levels of lactate dehydrogenase (LDH) as an indicator of glycolytic compensation as well as a spectrum of antioxidant enzymes as indexes of compensatory responses to oxidative stress. Although this treatment protocol causes extremely rapid, dramatic changes in left ventricular (LV) mass (~30% in <10 days), we find that the specific activity of mitochondrial parameters is tightly integrated into cardiac adaptation. However, profound differences in the relationship between mtDNA content and other mitochondrial elements provide insight into the mechanisms responsible for bioenergetic remodeling during hypertension.

METHODS

Animals and treatments. Male SHR (Charles River Laboratories, Montreal, PQ, Canada) were housed in pairs in a temperature-controlled room (22–24°C) with a 12:12-h light-dark cycle. Animals had access to food and water ad libitum, and all procedures were in accordance with the guidelines set out by the Canadian Council on Animal Care.

Antihypertensive drug treatment began at either 15 or 40 wk of age. Treatments (14 days) involved administration of the angiotensin-converting enzyme (ACE) inhibitor enalapril (30 $mg \cdot kg^{-1} \cdot day^{-1}$) in the drinking water and low-sodium chow (0.04%) to enhance the effects of enalapril on blood pressure. From treatment *day 6* to *day 14*, rats were allowed access to standard chow (0.4% Na^+) for 4 h/day to control blood pressure at values ~50% below pretreatment levels (T. M. Hale, T. L. Bushfield, and M. A. Adams, unpublished observation). A treatment cycle consisted of a 14-day period on enalapril, followed by a 14-day drug-free period. In one set of experiments, 40-wk-old animals were treated in this manner. In another set of experiments, 15-wk-old animals were treated with three consecutive cycles. Separate groups of age-matched SHR receiving standard chow and tap water served as time controls for the 19-, 27-, and 44-wk-old animals. Sampling of treated rats occurred either during drug treatment (at *day 10*) or after 2 wk of being drug free (*day 28*) (Fig. 1). Control SHR were killed at various points throughout the study.

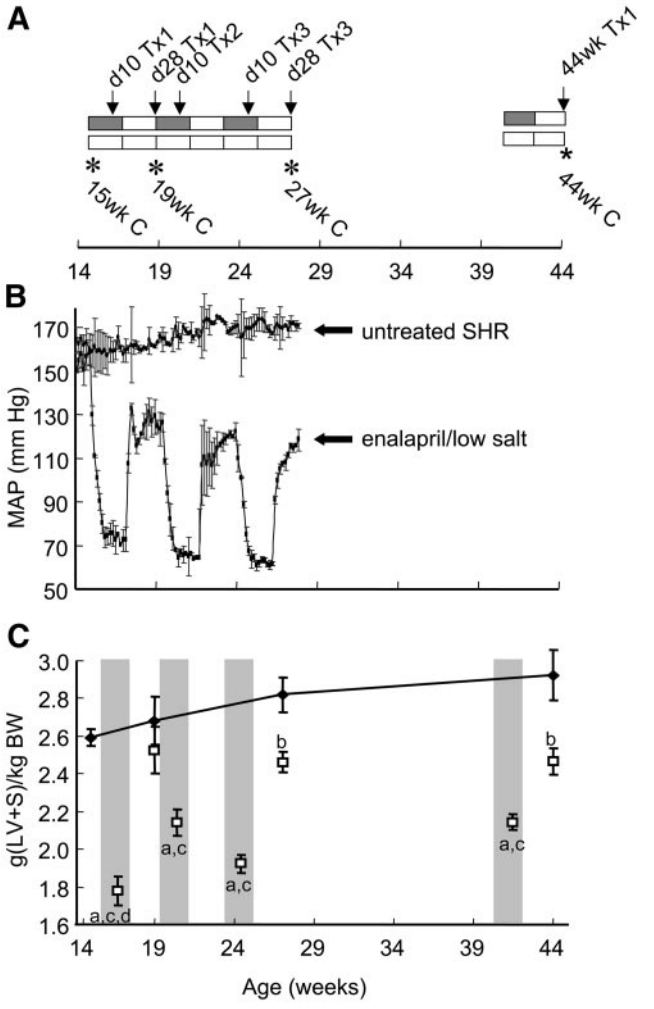

Fig. 1. Treatment profile of spontaneously hypertensive rats (SHR). *A*: bars represent 2-wk periods on enalapril treatment (gray bars) and off treatment (open bars). Arrows indicate sampling periods of treated animals. Asterisks represent sampling points for control animals. d, day; Tx, treatment; C, control. *B*: summary of the effects of enalapril and low-salt treatments on mean arterial blood pressure (MAP; measured as described in METHODS) of 4 rats (2 untreated, 2 treated). *C*: changes in left ventricular (LV) mass [including septum (S)] relative to body weight (BW) in control (♦) and enalapril-treated (□) animals (means ± SE, $n = 4–9$). Significant differences ($P < 0.05$) are denoted by letters: a, different from a 15-wk-old untreated rat; b, an age-matched time control; c, other treatment groups; d, all other time points. Gray bars represent periods of enalapril/low-salt treatment.

Assessment of mean arterial blood pressure recordings. Mean arterial blood pressure (MAP) was continuously monitored with a radiotelemetry data acquisition system (Data Sciences International, St. Paul, MN). Before implantation, all radiotransducers (model TA11PA-C40) were verified to be within ±4 mmHg of zero. At 13 wk of age, SHR (enalapril-low salt, $n = 2$; untreated control, $n = 2$) were anesthetized with ketamine-xylazine (70 mg/kg by intraperitoneal injection) and isofluorane (dosed to effect by inhalation). The fluid-filled telemetric catheter was introduced into the lower abdominal aorta such that the catheter was positioned ~1 cm below the left renal artery. The body of the transducer was sutured to the muscular layer of the abdominal wall to prevent movement of the device. All animals were allowed to recover for 10 days before baseline MAP was recorded. SHR were housed in individual cages that were placed on receivers (models RA1010 and RPC-1) that converted the radiotelemetric waveform into a digital signal. This information was then transmitted via a consolidation matrix (BCM100) to a computer-based acquisition system (Dataquest IV, version 2) located in an adjacent room. The arterial blood pressure for each animal was recorded at 150 Hz. Thirty seconds of MAP data was stored every 5 min. Twenty-four-hour MAP was calculated by clipping the data to within a threshold of 50–200 mmHg and averaging the 288 data points.

Enzyme assays and metabolite analyses. Hearts were excised from anesthetized rats (pentobarbital sodium, 1 mg/kg

body wt ip) and blotted dry. The extraneous tissue and atria were removed, and the right ventricle, LV, and septum were separated and weighed. For some hearts, core samples (2-mm diameter) were made from the septum and lateral wall of the LV. These cores were then cut in half to separate the endocardium from the epicardium. Samples were snap-frozen in liquid nitrogen and stored at −80°C for further analysis.

Powdered LVs were homogenized in 9 vols of homogenization buffer (20 mM HEPES pH 7.2, 1 mM EDTA, and 0.1% Triton X-100). Assays were performed on a Molecular Devices SpectraMAX Plus spectrophotometer thermostated to 37°C. The activities of cytochrome-*c* oxidase (COX), citrate synthase (CS), and LDH were measured with previously described protocols (20, 24). Assays for all other enzymes were optimized as described in detail below to ensure that neither substrates nor cofactors were limiting.

Total cellular superoxide dismutase (SOD) was assayed at 550 nm with the aerobic xanthine/xanthine oxidase (XO) system (9). The assay contained (in mM) 0.1 EDTA, 0.1 xanthine, 0.04 oxidized cytochrome *c*, and 20 U/ml XO in 50 potassium phosphate (pH 7.8). In the absence of homogenate, XO reduced cytochrome *c* at a rate of 0.08–0.12 absorbance units/min. One unit of total cellular SOD activity corresponds to the amount of homogenate required to inhibit the rate of cytochrome *c* reduction by 50%. We observed no reduction of cytochrome *c* in the absence of either XO or homogenate. The glutathione peroxidase (GPX) assay (16) contained (in mM) 1 glutathione, 0.15 NADPH, and 1.2 *tert*-butylhydroperoxide and 0.6 U/ml glutathione reductase in 50 potassium phosphate (pH 7.0). Activity was detected as the disappearance of NADPH at 340 nm. Catalase (1) was assayed with sonicated samples, by following the disappearance of hydrogen peroxide at 240 nm. The assay contained 20 mM hydrogen peroxide in 50 mM potassium phosphate (pH 7.0).

Quantitative-competitive polymerase chain reaction. A quantitative-competitive (QC)-PCR was established to measure LV mitochondrial DNA content. A 767-bp fragment of rat COX I was amplified at 58°C from a rat heart reverse transcriptase template with primers 5′-CAC AAA GAT ATC GGA ACC CTC-3′ and 5′-GTA ACT ACA TGT GAA ATA ATT CCA AA-3′ as follows: 10 mM Tris·HCl (pH 9.0), 1.5 mM $MgCl_2$, 50 mM KCl, 200 μM dNTPs, 200 ng/μl primers, and 2.5 U *Taq* polymerase (Qiagen). The resultant PCR product was cloned into pCR 2.1 (Invitrogen), and the plasmid was linearized by digestion at a unique *Hin*cII site within the insert. Ligation of a 188-bp blunt-end fragment allowed for the generation of a plasmid containing a 955-bp competitor template. The identity of the competitor construct was confirmed by sequencing. An optimal range of ratios of LV homogenate to competitor template was initially determined to avoid unequal competition during the QC-PCR reaction. This concentration was established by varying the amount of homogenate per reaction in the presence of a constant amount of competitor template. The PCR reaction contained 30 mU CS, 10 mM Tris·HCl (pH 9.0), 2.5 mM $MgCl_2$, 50 mM KCl, 0.2 mM dNTPs, 9.7 ng/μl forward primer, 14.44 ng/μl reverse primer, and 1.5 U *Taq* polymerase. PCR conditions were as follows: 2 min at 40°C, initial denaturation for 5 min at 95°C, subsequent denaturations for 15 s at 95°C, annealing for 1 min at 62°C, extension for 1 min at 72°C, and final extension at 72°C for 10 min. The PCR was run for 30 cycles, with [α-^{32}P]dCTP added for the last five cycles. PCR products were resolved on 6% polyacrylamide gels and dried, and the signal strength was quantified with a phosphorimager (Bio-Rad).

Immunoblotting and protein analyses. Protein from roughly 5 mg of powdered LV was extracted for 15 min on ice in RIPA buffer. Equal amounts of total protein were denatured, loaded onto a 12% SDS-polyacrylamide gel, and electrophoresed at 120 V for 1.5 h. Gels were then electroblotted (Mini-protean system, Bio-Rad) for 2 h at 50 V onto nitrocellulose membrane (Zymotech) and blocked in 50 mM Tris·HCl (pH 7.4), 150 mM NaCl containing 0.05% Tween 20 (TBS-T) supplemented with 5% low-fat skim milk powder. Membranes were incubated overnight at 4°C in TBS-T containing 2% low-fat skim milk powder and the primary antibody of interest. Rabbit polyclonal antibodies directed against Cu/Zn and MnSOD (StressGen Biotechnologies, Victoria, BC, Canada), COX II (kind gift from Dr. E. A. Shoubridge, Montreal Neurological Institute, Montreal, Canada), Tfam (kind gift from Dr. N.-G. Larsson, Karolinska Hospital, Stockholm, Sweden), and cytochrome *c* (Santa Cruz Biotechnologies, Santa Cruz, CA) and mouse monoclonal anti-COX I, COX IV, and NADH dehydrogenase subunit 1 (ND1) (Molecular Probes) antibodies were all used at 1:1,000 dilutions. Rabbit polyclonal anti-catalase (Rockland Immunochemicals) and anti-actin (Sigma) antibodies and a monoclonal anti-porin antibody (Calbiochem) were used at 1:25,000, 1:5,000, and 1:2,000 dilutions, respectively. After a 1-h incubation at room temperature with either secondary anti-mouse (1:10,000; Pierce) or anti-rabbit (1:2,500; Promega) horseradish peroxidase antibodies, immunoreactive proteins were visualized with luminol-enhanced chemiluminescence (Amersham Pharmacia Biotech).

RNA isolation, Northern analysis, and cDNA constructs. Total RNA was purified from guanidinium thiocyanate extracts with an acid-phenol protocol. RNA was quantified in triplicate spectrophotmetrically, denatured, and fractionated with a standard 1% agarose-formaldehyde gel system. cDNAs for catalase, MnSOD, Cu/ZnSOD, LON protease, Tfam, rat hypertensive protein (a fuzzy onion homolog), uncoupling protein-2, dynamin-like protein, and synaptojanin-2α were amplified from an appropriate reverse transcriptase template in 10 mM Tris·HCl (pH 9.0), 1.5 mM $MgCl_2$, 50 mM KCl, 200 μM dNTP, 200 ng/μl primers, and 2.5 U *Taq* polymerase (Qiagen) (Table 1). PCR conditions were as follows: initial denaturation at 95°C for 60 s, subsequent denaturations at 95°C for 30 s, annealing for 90 s, extension at 72°C for 90 s, and a final extension at 72°C for 10 min. All other probes for mtDNA- and nuclear-encoded mRNA species were obtained as previously described (8, 20). Blots were corrected for loading differences with a probe for α-tubulin mRNA.

Membranes were prehybridized and hybridized at 65°C in a Hybaid minihybridization oven (Interscience) in modified Church's buffer (0.5 M sodium phosphate pH 7.2, 10 mM EDTA, and 7% SDS). Membranes were washed twice at room temperature for 15 min with 2× SSC-0.1% SDS and twice at 50°C for 15 min with 0.1× SSC-0.1% SDS. Blots were phosphorimaged, and relative signal strength was quantified with Imagequant software (Molecular Dynamics).

Statistical analyses. For all parameters, significant differences ($P < 0.05$) between control and enalapril-treated SHR were detected with one-way ANOVA and identified post hoc with the Tukey-Kramer honestly significant difference test. Two-way ANOVAs were also used to test for significant differences ($P < 0.05$) between enalapril-treated SHR and specific age-matched controls as a function of treatment and time.

RESULTS

Effects on LV mass. SHR treated with enalapril exhibited a rapid and significant reduction in LV mass

Table 1. *Primer sequence, annealing temperature, and RT template source designed for amplifying rat nuclear DNA gene products*

GENE	Forward Primer (5′–3′)	Reverse Primer (5′–3′)	T, °C	RT Template	Size, bp
Tfam (U63858)	cttgtctgtattccgaagtg	tgctcagagatgtctccg	48	skeletal muscle*	631
MnSOD (Z18857)	acctgccttacgactatgg	ccagttgattacattccaaat	62	skeletal muscle*	542
Catalase (M11670)	atgtcctgaccaccgg	cctcctcattcaacacctt	58	skeletal muscle*	1,291
Cu/ZnSOD (M21060)	acttcgagcagaaggca	cagcatttccagtctttgtac	62	skeletal muscle*	366
RHP (U41803)	accgtgaaccagctagccccatg	tcgatccaccacgcctagctcatc	60	skeletal muscle*	419
LON protease (U02389)	ttggttgagctgctgagaagg	gaggagtggttgtccagcag	55	HEK 293	914
Synaptojanin-2α (U90312)	cttagcggatgagtttggtca	tctacgggtgtcagtctctgg	55	skeletal muscle*	347
DLP (AF019043)	ccttagaatctgttgatccac	ttgtctcgtgatacagctgaa	51	skeletal muscle*	478
UCP-2 (AB006613)	aaggccaccgatgtgccc	ttgtaggcttcgacagtgctct	60	ASMC†	487

Nos. in parentheses are GENBank accession nos. DLP, dynamin-like protein; RHP, rat hypertensive protein; UCP-2, uncoupling protein 2; SOD, superoxide dismutase. *Total RNA from Sprague-Dawley rat skeletal muscle; †total RNA from aortic smooth muscle cell (ASMC) primary cultures.

expressed per kilogram of body weight (Fig. 1). In contrast, LV mass remained a fixed proportion of body weight over the entire experimental time period in control SHR. Although the extent of LV regression in enalapril-treated SHR was significantly greater during the first treatment cycle, LV mass per kilogram of body weight returned toward that of age-matched controls after 14 days of treatment. Additional treatment cycles further reduced LV mass per kilogram of body weight. The steady-state LV mass at the end of each cycle remained depressed relative to age-matched controls.

Effects on enzyme specific and total activities. The activities of metabolic enzymes were measured to assess changes in cardiac bioenergetics associated with enalapril-mediated LV remodeling. To ensure that the interpretation of such results was not confounded by significant transmural differences in enzymatic distribution (35, 36), activities were initially measured in the endocardium and epicardium of septum and LV. No significant differences were observed between the endocardium and epicardium in either the septum or LV of enalapril-treated and time-control SHR for bioenergetic enzymes (Table 2). Whole LV was therefore used as starting material for all further analyses.

Although specific activity is an appropriate parameter when considering functional consequences of enzymatic changes, total activity is more meaningful when considering the mechanistic basis because it takes into account the impact of changes in ventricular mass. Although specific activities (U/g LV) of most enzymes were constant, significant changes in total enzymatic content (U/LV) were observed with treatment and age (Figs. 2 and 3). Thus changes in enzyme synthesis/degradation were required during LV remodeling. The specific activities of COX, CS, and LDH (U/g LV) were preserved over a fairly narrow range regardless of treatment duration or organismal age (Figs. 2 and 3). No significant effects of enalapril treatment were observed for LDH. Enalapril effects on COX and CS were subtly different, with CS activity essentially remaining a fixed activity per gram of LV whereas prolonged enalapril treatment resulted in modest but significant increases in COX activity (Fig. 2, *A* and *B*).

Effects on mitochondria. Throughout the enalapril treatment protocol mitochondrial enzymes largely demonstrated constant specific activity. In contrast, mtDNA content (copies per LV) was constant (Fig. 2*C*), such that its "specific activity" (mtDNA copy number/g LV) varied approximately twofold with LV mass (Fig. 2*C*). Off-treatment and control SHR had comparable mtDNA contents and specific activities, with the total number of copies of mtDNA increasing by ~10%/wk in untreated SHR as a function of age (Fig. 2*C*).

Unlike the situation with mtDNA, RNA and protein levels of mitochondrial- (COX I, II) and nuclear-encoded (COX IV) COX subunits were unchanged with either age or drug treatment (Fig. 4). Similarly, the levels of two other bioenergetic proteins, the ND1 subunit of complex I and cytochrome *c*, the mobile electron carrier between complexes III and IV, were unaffected (Fig. 4*C*).

Table 2. *Enzyme activity ratios from endocardium and epicardium of septum and left ventricle of control and enalapril-treated SHR*

Activity Ratio (Endo/Epi)	COX	CS	LDH	SOD	GPX	Catalase
Control						
LV	1.02 ± 0.13	1.02 ± 0.10	1.20 ± 0.11	1.10 ± 0.19	0.82 ± 0.14	0.84 ± 0.02*
S	0.92 ± 0.17	1.15 ± 0.13	1.04 ± 0.08	0.92 ± 0.11	0.93 ± 0.19	1.12 ± 0.14
Treated						
LV	0.99 ± 0.11	0.99 ± 0.06	0.94 ± 0.07	1.40 ± 0.08*	0.75 ± 0.08*	1.00 ± 0.08
S	1.01 ± 0.28	1.00 ± 0.16	0.93 ± 0.19	1.37 ± 0.14	0.80 ± 0.22	1.04 ± 0.15

Values are means ± SE for $n = 5$ experiments. SHR, spontaneously hypertensive rats; COX, cytochrome-*c* oxidase; CS, citrate synthase; LDH, lactate dehydrogenase; GPX, glutathione peroxidase; LV, left ventricle; S, septum. *$P < 0.05$, denotes ratio significantly different from 1.

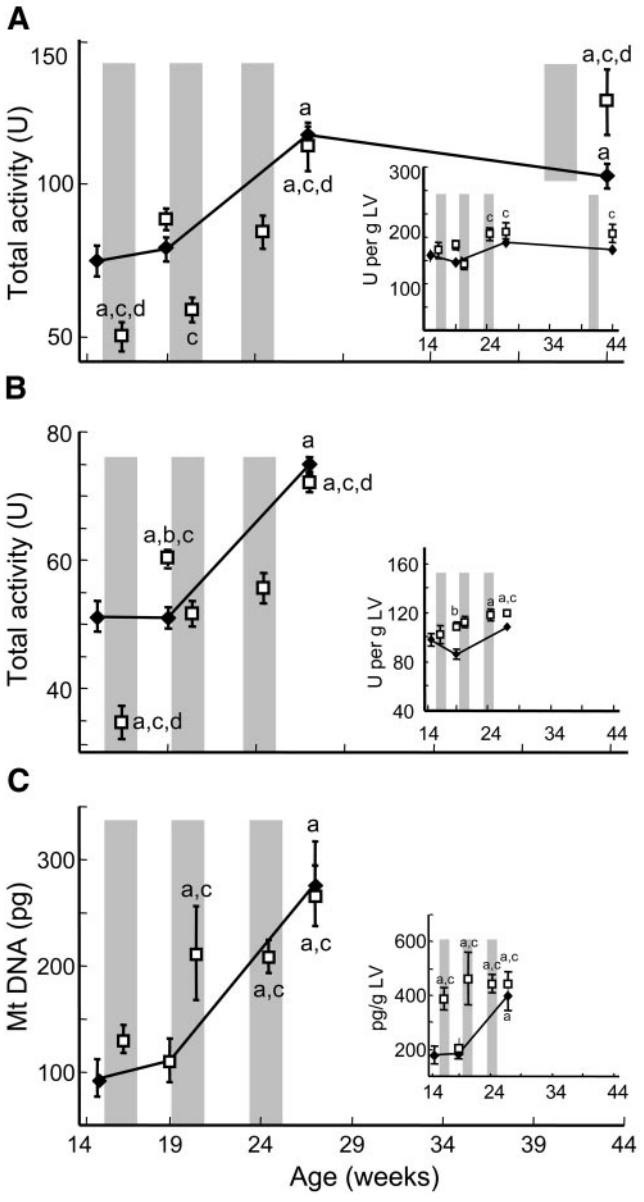

Fig. 2. Changes in the activities of mitochondrial enzymes cytochrome-*c* oxidase (COX, *A*), citrate synthase (CS, *B*), and mtDNA (*C*) in LV of control (♦) and enalapril-treated (□) rats. *Insets* in each panel reflect specific activity (U/g LV). Main panels are total activities, which is the product of specific activity (U/g) × LV mass (g/kg body mass). All data are presented as means ± SE (n = 4–11). Symbols denoting significant differences are as in Fig. 1.

Discordant changes in mitochondrial enzymes and mtDNA copy number prompted us to measure the mRNA levels of several factors known to collaborate in the regulation of mtDNA expression. Tfam transcript and protein levels were unaffected by enalapril treatment (Fig. 4). Similarly, no changes were observed in the mRNA levels of LON protease (Fig. 4).

We also investigated possible changes in the mRNA levels of proteins implicated in the maintenance of the mitochondrial reticulum. We found no changes in the transcript levels of proteins involved in mitochondrial fusion (rat hypertensive protein, a putative homolog of fuzzy onion) or fission (dynamin-like protein or the inositol 5′-phosphatase synaptojanin-2α) (Fig. 4).

Antioxidant enzyme activities and RNA. As with bioenergetic enzymes there were no systematic transmural differences in antioxidant enzyme levels (Table 2). The LV specific activities of SOD decreased marginally with age but were unaffected by treatment (Fig. 3). Similarly, protein levels of MnSOD and Cu/ZnSOD were unaffected by treatment (Fig. 5). In contrast, catalase-specific activity (Fig. 3) and protein levels (Fig. 5) increased with age and enalapril treatment. There was no effect of age or treatment on mRNA levels for catalase, MnSOD, or Cu/ZnSOD.

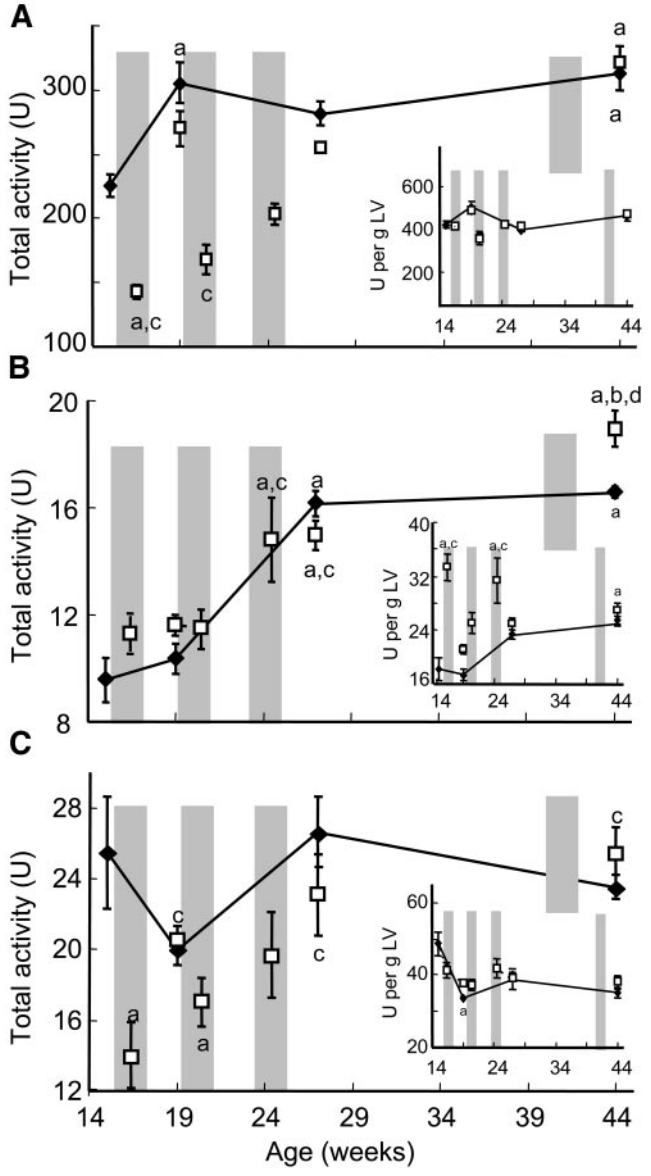

Fig. 3. Changes in the enzyme activities of lactate dehydrogenase (LDH, *A*), catalase (*B*), and total cellular superoxide dismutase (SOD, *C*) in control (♦) and enalapril-treated (□) animals. Main panels and *insets* are as in Fig. 2. Symbols denoting significant differences are as in Fig. 1.

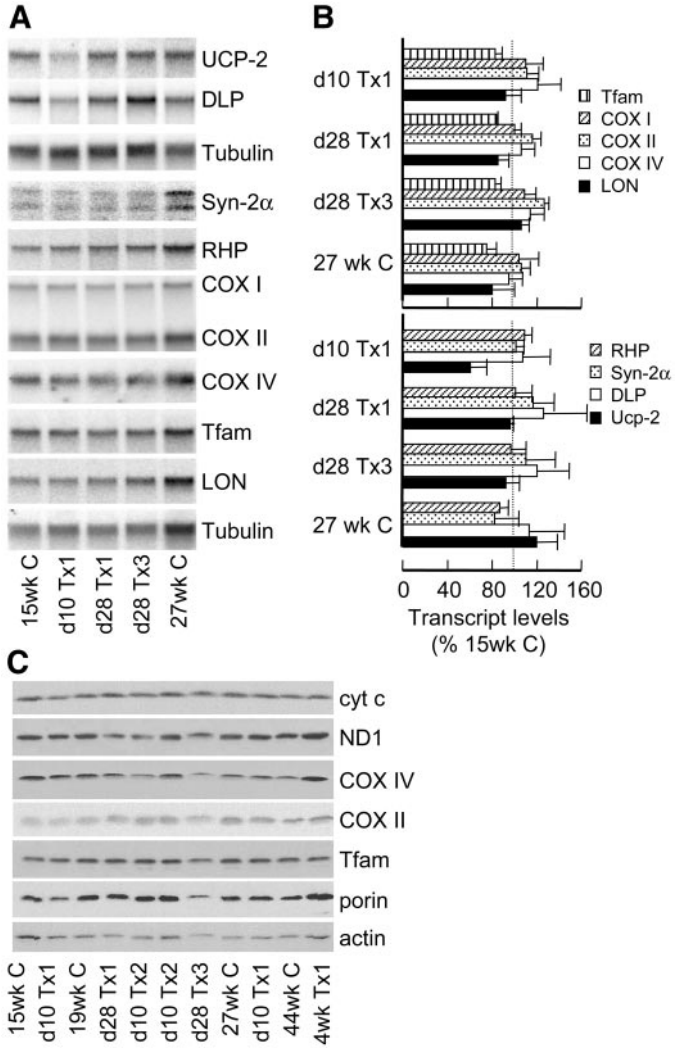

Fig. 4. Changes in mtRNA and proteins. *A*: representative Northern blots for a series of gene products involved in control of mitochondrial structure and function. *B*: summary of Northern analyses normalized to α-tubulin and expressed relative to 15-wk time controls (n = 3). RHP, rat hypertensive protein (a rat fuzzy onion homolog); DLP, dynamin-like protein; Syn-2α, synaptojanin-2α; UCP, uncoupling protein. *C*: Western blot analysis of changes in steady-state levels of select bioenergetic proteins.

DISCUSSION

Mitochondrial changes during hypertrophy and regression. Mitochondria play a critical role in maintaining normal heart function by producing most of the ATP needed in energy metabolism and by generating ROS at levels that modulate signal transduction. Although low levels of mitochondrial ROS production exert a regulatory role within the cell, hypertensive animals exhibit a broad range of dysfunction that could enhance the rate of ROS generation and, as a result, their cytotoxic as opposed to regulatory effects. Mitochondrial abnormalities include defects in Ca^{2+} handling, phosphate transport, and ATP synthesis/export (3, 4, 35, 36). Thus maintenance of mitochondrial structure and function is an important element of cardiac adaptation.

We used the SHR model to address the nature of bioenergetic remodeling during cardiac adaptation that accompanies both hypertension and antihypertensive treatment with the ACE inhibitor enalapril. While we focus our discussion on the role of blood pressure manipulation on cardiac adaptation, we cannot address the role of other effectors that could contribute to control of mitochondrial gene expression. In particular, changes in insulin and insulin sensitivity, which may participate in hypertensive remodeling, are often accompanied by changes in mitochondria (2). Enalapril and low-salt treatment resulted in a rapid reversal of cardiac hypertrophy (~30% by 10 days). Enalapril-mediated changes in ventricular mass were somewhat reversible, although repeated treatment cycles led to sustained improvements in both MAP and LV mass.

Despite the changes in ventricular mass in response to this complex treatment protocol, the specific activities of mitochondrial (COX, CS) and glycolytic (LDH) enzymes were highly preserved. Conservation of the specific activity of bioenergetic enzymes was seen across heart compartments and transmural regions and throughout aging. Collectively, these observations suggest that bioenergetic changes are well integrated into both rapid (i.e., enalapril + low salt) and slow (i.e., age-related hypertrophy) phases of cardiac adaptation. These changes in bioenergetics are consistent with a general model in support of maintenance of LV function during hypertension and its treatment (see, e.g., Ref. 8). The relative importance of control of synthesis and degradation in achieving these mitochondrial changes is largely unknown, although our data provide some insight into the possibilities.

During off-treatment periods, mitochondrial enzyme content increased rapidly to preserve specific activities as ventricular hypertrophy occurred. In differentiating C2C12 myocytes, another model of mitochondrial proliferation, a threefold increase in COX activity over a 14-day period was accompanied by a twofold increase in mitochondrially encoded COX mRNA levels (24). If this relationship between enzyme activity and RNA levels held in cardiomyocytes, an increase in total COX activity over roughly the same time period (~60% in 14 days) could be achieved with relatively modest increases in COX mRNA levels (~40%). Thus our relatively broad time course may have precluded detection of periods of elevated mRNA for mitochondrial enzymes. However, recent studies have shown that ANG II signaling leads to activation of protein synthesis through dephosphorylation of eEF2, an elongation factor involved in translation (14). As a result, the "recovery" of ANG II signaling as off-treatment SHR rehypertrophy need not be restricted to effects on transcription, and in fact, both enhanced rates of protein synthesis and reduced rates of protein degradation are known to contribute to the coordinated increase in mitochondrial content that accompanies cardiac hypertrophy in response to aortic banding (46).

ROS, respiratory gene expression, and cardiac hypertrophy. ROS have frequently been implicated as participants in regulatory pathways associated with the

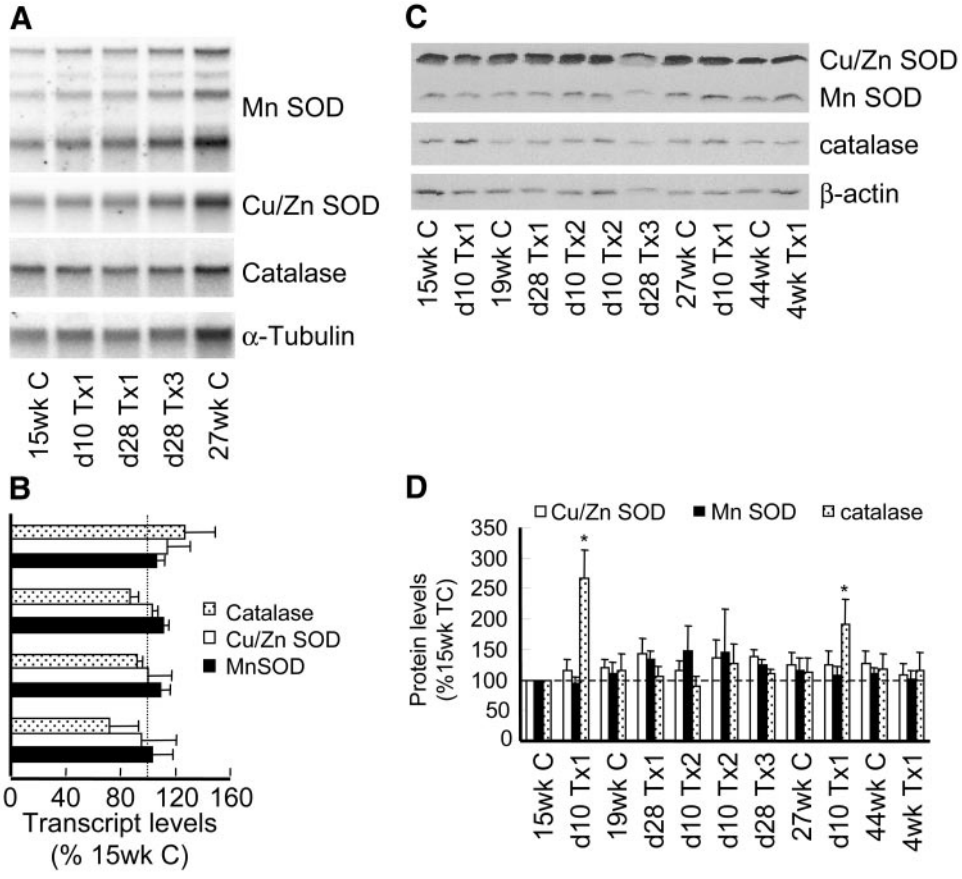

Fig. 5. Changes in antioxidant enzyme RNA and proteins. *A*: representative Northern blots summarized in *B*. *C*: representative Western blots summarized in *D* after normalization to actin and expressed relative to 15-wk time controls ($n = 4$).

hypertrophic response (13, 30, 42). Antioxidants and antioxidant enzymes inhibit the regulatory effects of ANG II on Ras/Raf/extracellular signal-regulated kinase (37) and AP-1 (31) signaling pathways. Enhanced mitochondrial H_2O_2 production has also been shown to alter cellular metabolism by increasing c-Jun NH_2-terminal kinase (JNK) activity (25). JNK is a downstream target of AT_1-dependent signaling (19) and regulates AP-1 activity via c-Jun. Altered mitochondrial ROS production is thought to modulate the activity of ROS-sensitive transcription factors and kinases, thereby allowing for changes in nuclear gene expression (29). Whereas stressors that lead to enhanced ROS production can increase expression of respiratory genes (38), it is not clear whether ROS are a plausible effector of changes in mitochondrial enzyme synthesis during ANG II-dependent hypertensive hypertrophy.

Because AP-1 interacts with nuclear respiratory factor-1 to transcriptionally regulate cytochrome *c* expression (43, 44), JNK may facilitate coordinated changes in the contractile apparatus and mitochondrial content in response to hypertensive stimuli. However, our data argue against a regulatory role for ROS in the observed increases in mitochondrial enzymes. The activity of catalase was previously shown to increase in SHR after a 30-min infusion with 25 μM H_2O_2 (10). In the present study, the highest specific activity of catalase was observed during periods of mitochondrial regression (i.e., enalapril treatment) as opposed to proliferation. Enalapril-mediated increases in catalase are consistent with other observations that suggest that enalapril treatment leads to enhanced antioxidant capacity as a result of experiencing some degree of oxidative stress (11, 12).

Mitochondrial losses during ventricular regression. Unlike control of protein turnover during hypertrophy, the relative importance of protein synthesis versus degradation in mediating mitochondrial regression is less understood. During enalapril treatment, LV regression was accompanied by parallel losses in mitochondrial enzyme content (U/LV), but mtDNA content (copies/LV) was unaffected. Discordant changes in the levels of mitochondrial parameters suggest that although reduced protein synthesis could play a role, enhanced degradation is likely the dominant mechanism of mitochondrial regression. Whether degradation is mediated by intramitochondrial proteases or organellar degradation via autophagy is unclear. Although both pathways are typically considered to be involved in organellar maintenance, it is unlikely that the coordinate activity of intramitochondrial proteases could account for the relatively rapid (~30% in 10 days) and largely stoichiometric reductions in bioenergetic enzymes.

Organellar degradation via autophagy relies on the activity of several proteins involved in reticulum maintenance and their ability to interact with outer mitochondrial membrane proteins to promote either fission

or fusion (21). With the discovery of fuzzy onion, dynamin-like protein, and a suite of other proteins involved in reticulum maintenance, there has been much interest in the control of mitochondrial autophagy (21, 45). However, the fundamental mechanisms by which specific regions of the mitochondrial reticulum are liberated and degraded are relatively unknown. Although enalapril treatment did not affect mRNA levels of proteins implicated in reticulum fusion (i.e., rat hypertensive protein) and fission (i.e., dynamin-like protein and synaptojanin-2α), little is known about how their levels/activities are regulated. Although autophagy would account for stoichiometric reductions in mitochondrial enzymes, retention of mtDNA during enalapril treatment would appear to be somewhat of a paradox. However, recent studies have shown that Mmm1p, an outer mitochondrial membrane protein, has dual roles in reticulum maintenance and organization of mtDNA aggregation (17). This presents the possibility that proteins such as Mmm1p could participate in determining selectivity of mitochondrial autophagy.

mtDNA and mitochondrial gene expression. Control of mtDNA copy number and expression is thought to involve both nucleocytosolic and intramitochondrial controls (23, 34). Changes in mtDNA expression can arise in many diseases, often as a result of mutations (40). In particular, diabetes can be accompanied by losses in mtDNA in skeletal muscle by an unknown mechanism (2). We saw no age- or treatment-dependent change in the expression of two proteins implicated in control of mtDNA expression/replication, Tfam and LON protease (23). In this SHR model mtDNA copy number increased with age (2.5-fold over 14 wk), but treatment regimes did not affect the total mtDNA copy number. When ventricular mass decreased (while on enalapril) or increased (off enalapril), the specific activity of mtDNA changed in parallel. However, there was no corresponding change in the steady-state levels of mtDNA-encoded gene products. Although there is a general relationship between mtDNA copy number and mtDNA expression (23), we found that changes seen during enalapril-induced bioenergetic remodeling altered this relationship by as yet unidentified mechanisms.

Perspectives. We demonstrated that despite pronounced LV regression, the specific activities of bioenergetic (COX, CS, and LDH) and superoxide-scavenging (Cu/Zn SOD and MnSOD) enzymes were largely preserved irrespective of treatment duration, organismal age, or transmural region. The significant changes in catalase and mtDNA copy number per gram of LV argue that active mitochondrial remodeling resulted not only in the removal of selected mitochondrial elements but also in enhanced H_2O_2 production. The relative contributions of synthetic and degradative pathways and the associated signal transduction pathways that can account for the observed effects of enalapril treatment are currently being investigated.

This work was funded by the Heart and Stroke Foundation of Ontario through Grants-in-Aid A-4120 and T4841 (to C. D. Moyes) and Fellowships (to S. C. Leary) and a Canadian Institutes of Health Research grant (to M. A. Adams).

REFERENCES

1. **Aebi H.** Catalase. In: *Methods of Enzymatic Analysis*, edited by Bergmeyer HU. New York: Academic, 1974, p. 673–678.
2. **Antonetti DA, Reynet C, and Kahn CR.** Increased expression of mitochondrial-encoded genes in skeletal muscle of humans with diabetes mellitus. *J Clin Invest* 95: 1383–1388, 1995.
3. **Atlante A, Abruzzese F, Seccia TM, Vulpis V, Doonan S, Pirrelli A, and Marra E.** Changes in enzyme levels in hypertensive heart tissue. *Biochem Mol Biol Int* 37: 983–990, 1995.
4. **Atlante A, Seccia TM, Pierro P, Vulpis V, Marra E, Pirrelli A, and Passarella S.** ATP synthesis and export in heart left ventricle mitochondria from spontaneously hypertensive rat. *Int J Mol Med* 1: 709–716, 1998.
5. **Binda D, Nicod L, Viollon-Abadie C, Rodriguez S, Berthelot A, Coassolo P, and Richert L.** Strain differences (WKY, SPRD) in the hepatic antioxidant status in rat and effect of hypertension (SHR, DOCA). Ex vivo and in vitro data. *Mol Cell Biochem* 218: 139–146, 2001.
6. **Bota DA and Davies KJA.** Protein degradation in mitochondria: implications for oxidative stress, aging and disease: a novel etiological classification of mitochondrial proteolytic disorders. *Mitochondrion* 1: 33–50, 2001.
7. **Chen L, Tian X, and Song L.** Biochemical and biophysical characteristics of mitochondria in the hypertrophic hearts from hypertensive rats. *Chin Med J (Engl)* 108: 361–366, 1995.
8. **Childs TJ, Adams MA, and Mak AS.** Regression of cardiac hypertrophy in spontaneously hypertensive rats by enalapril and the expression of contractile proteins. *Hypertension* 16: 662–668, 1990.
9. **Crapo JD, McCord JM, and Fridovich I.** Preparation and assay of superoxide dismutases. *Methods Enzymol* 53: 382–393, 1978.
10. **Csonka C, Pataki T, Kovacs P, Muller SL, Schroeter ML, Tosaki A, and Blasig IE.** Effects of oxidative stress on the expression of antioxidant defense enzymes in spontaneously hypertensive rat hearts. *Free Radic Biol Med* 29: 612–619, 2000.
11. **De Cavanagh EM, Ferder L, Carrasquedo F, Scrivo D, Wassermann A, Fraga CG, and Inserra F.** Higher levels of anti-oxidant defences in enalapril-treated versus no-enalapril-treated hemodialysis patients. *Am J Kidney Dis* 34: 445–455, 1999.
12. **De Cavanagh EM, Inserra F, Ferder L, and Fraga CG.** Enalapril and captopril enhance glutathione-dependent antioxidant defenses in mouse tissues. *Am J Physiol Regulatory Integrative Comp Physiol* 278: R572–R577, 2000.
13. **Dhalla NS, Temsah RM, and Netticada T.** Role of oxidative stress in cardiovascular diseases. *J Hypertens* 18: 655–673, 2000.
14. **Everett AD, Stoops TD, Nairn AC, and Brautigan D.** Angiotensin II regulates phosphorylation of translation elongation factor-2 in cardiac myocytes. *Am J Physiol Heart Circ Physiol* 281: H161–H167, 2001.
15. **Ferder L, Romano LA, Ercole LB, Stella I, and Inserra F.** Biomolecular changes in the ageing myocardium: the effect of enalapril. *Am J Hypertens* 11: 1297–1304, 1998.
16. **Flohe L and Gunzler WA.** Assays of glutathione peroxidase. *Methods Enzymol* 105: 114–21, 1984.
17. **Hobbs AEA, Srinivasan M, McCaffery JM, and Jensen RE.** Mmm1p, a mitochondrial outer membrane protein, is connected to mitochondrial DNA (mtDNA) nucleoids and required for mtDNA stability. *J Cell Biol* 152: 401–410, 2001.
18. **Kim S and Iwao H.** Molecular and cellular mechanisms of angiotensin II-mediated cardiovascular and renal diseases. *Pharmacol Rev* 52: 11–34, 2001.
19. **Kudoh S, Komura I, Mizuno T, Yamazaki T, Zou Y, Shiojima I, Takekoshi N, and Yazaki Y.** Angiotensin II stimulates c-Jun NH_2-terminal kinase in cultured myocytes of neonatal rats. *Circ Res* 82: 244–250, 1997.
20. **Leary SC, Battersby BJ, Hansford RG, and Moyes CD.** Interactions between bioenergetics and mitochondrial biogenesis. *Biochim Biophys Acta* 1365: 522–530, 1998.

21. **Luzikov VN.** Quality control: from molecule to organelles. *FEBS Lett* 448: 201–205, 1999.
22. **Makino N, Sugano M, Hata T, Taguchi S, and Yanaga T.** Chronic low-dose treatment with enalapril induced cardiac regression of left ventricular hypertrophy. *Mol Cell Biochem* 163/164: 239–245, 1996.
23. **Moraes CT.** What regulates mitochondrial DNA copy number in animal cells? *Trends Genet* 17: 199–205, 2001.
24. **Moyes CD, Mathieu-Costello OA, Tsuchiya N, Filburn C, and Hansford RG.** Mitochondrial biogenesis during cellular differentiation. *Am J Physiol Cell Physiol* 272: C1345–C1351, 1997.
25. **Nemoto S, Takeda K, Yu ZX, Ferrans VJ, and Finkel T.** Role of mitochondrial oxidants as regulators of cellular metabolism. *Mol Cell Biol* 20: 7311–7318, 2000.
26. **Nishio ML, Ornatsky OI, Craig EE, and Hood DA.** Mitochondrial biogenesis during pressure overload induced cardiac hypertrophy in adult rats. *Can J Physiol Pharmacol* 73: 630–637, 1995.
27. **Nishio ML, Ornatsky OI, and Hood DA.** Effects of hypothyroidism and aortic constriction on mitochondria during cardiac hypertrophy. *Med Sci Sports Exerc* 27: 1500–1508, 1995.
28. **Nunez E, Hosoya K, Susic D, and Frohlich ED.** Enalapril and losartan reduced cardiac mass and improved coronary haemodynamics in SHR. *Hypertension* 29: 519–524, 1997.
29. **Poyton RO and McEwen JE.** Cross talk between nuclear and mitochondrial genomes. *Annu Rev Biochem* 65: 563–607, 1996.
30. **Purcell NH, Tang G, Yu C, Mercurio F, DiDonato JA, and Lin A.** Activation of NFκB is required for hypertrophic growth of pituitary rat neonatal ventricular cardiomyocytes. *Proc Natl Acad Sci USA* 98: 6668–6673, 2001.
31. **Puri PL, Avantaggiati ML, Burgio VL, Chirillo P, Collepardo D, Natoli G, Balsano C, and Levrero M.** Reactive oxygen intermediates mediate angiotensin II-induced cJun-cFos heterodimer DNA binding activity and proliferative hypertrophic responses in myogenic cells. *J Biol Chem* 270: 22129–22134, 1995.
32. **Ruwhof C and van der Laarse A.** Mechanical stress-induced cardiac hypertrophy: mechanisms and signal transduction pathways. *Cardiovasc Res* 47: 23–37, 2000.
33. **Sanbe A, Tanonaka K, Kobayashi R, and Takeo S.** Effects of long-term therapy with ACE inhibitors, captopril, enalapril and trandolapril, on myocardial energy metabolism in rats with heart failure following myocardial infarction. *J Mol Cell Cardiol* 27: 2209–2222, 1995.
34. **Scarpulla RC.** Nuclear control of respiratory chain expression in mammalian cells. *J Bioenerg Biomembr* 29: 109–119, 1997.
35. **Seccia TM, Atlante A, Vulpis V, Marra E, Passarella S, and Pirrelli A.** Mitochondrial energy metabolism in the left ventricular tissue of spontaneously hypertensive rats: abnormalities in both adenine nucleotide and phosphate translocators and enzyme adenylate-kinase and creatine-phosphokinase activities. *Clin Exp Hypertens* 20: 345–358, 1998.
36. **Seccia TM, Atlante A, Vulpis V, Marra E, Passarella S, and Pirrelli A.** Abnormal transport of inorganic phosphate in left ventricular mitochondria from spontaneously hypertensive rats. *Cardiologia* 44: 719–725, 1999.
37. **Shih NL, Cheng TH, Loh SH, Cheng PY, Wang DL, Chen YS, Liu SH, Liew CC, and Chen JJ.** Reactive oxygen species modulate angiotensin II-induced B-myosin heavy chain gene expression via Ras/Raf/extracellular signal-regulated kinase pathway in neonatal rat cardiomyocytes. *Biochem Biophys Res Commun* 283: 143–148, 2001.
38. **Suzuki H, Kumagai T, Goto A, and Sugiura T.** Increase in intracellular hydrogen peroxide and upregulation of a nuclear respiratory gene evoked by impairment of mitochondrial electron transfer in human cells. *Biochem Biophys Res Commun* 249: 542–545, 1998.
39. **Tokoro T, Ito H, and Suzuki T.** Alterations in mitochondrial DNA and enzyme activities in hypertrophied myocardium of stroke-prone SHRS. *Clin Exp Hypertens* 18: 595–606, 1996.
40. **Wallace DC.** Mouse models for mitochondrial disease. *Am J Med Genet* 106: 71–93, 2001.
41. **Williams RS.** Cardiac involvement in mitochondrial diseases and vice versa. *Circulation* 91: 1266–1268, 1995.
42. **Wolfe G.** Free radical production and angiotensin. *Curr Hypertens Rep* 2: 167–173, 2000.
43. **Xia Y, Buja LM, and McMillin JB.** Activation of the cytochrome *c* gene by electrical stimulation in neonatal rat cardiac myocytes. Role of NRF-1 and c-Jun. *J Biol Chem* 273: 12593–12598, 1998.
44. **Xia Y, Buja LM, Scarpulla RC, and McMillin JB.** Electrical stimulation of neonatal cardiomyocytes results in the sequential activation of nuclear genes governing mitochondrial proliferation and differentiation. *Proc Natl Acad Sci USA* 94: 11399–11404, 1997.
45. **Yaffe MP.** The machinery of mitochondrial inheritance and behaviour. *Science* 283: 1493–1496, 1999.
46. **Zak R, Martin AF, Reddy MK, and Rabinowiz M.** Control of protein balance in hypertrophied cardiac muscle. *Circ Res* 38: I145-I150, 1976.